DEMISABILITY OF GFRP AND CFRP COMPONENTS OF REENTERING ORBITAL DEBRIS: PHASE I TEST RESULTS

Benton R. Greene[(1)], Christopher M. Sanchez[(2)]

[(1)] Jacobs JETS Contract, NASA Johnson Space Center, Mail Code XI4-9E, Houston, TX 77058, USA, Email:benton.r.greene@nasa.gov

[(2)] Applied Research Associates, Inc., 4300 San Mateo Blvd NE, Suite A-220, Albuquerque, NM 87110, USA, Email: csanchez@ara.com

ABSTRACT

Observations of surviving reentry debris on the ground and research performed by Hyperschall Technologie Göttingen (HTG) [1] indicated that significantly more glass fiber-reinforced polymer (GFRP) and carbon fiber-reinforced polymer (CFRP) components survive reentry than current models predict. NASA's Orbital Debris Program Office conducted a series of tests to evaluate the accuracy of material demise models for reentering orbital debris used in NASA's Object Reentry Survival Analysis Tool (ORSAT) and Debris Assessment Software (DAS).

Testing is planned in a multi-phase series to allow for quick quantification of results as well as refinement of methods resulting from lessons learned during early phases. The Phase 1 tests discussed here validated ORSAT models for homogeneous metals, provided an efficient quantification of composite material demisability properties like mass loss rate and overall time to demise, and identified potential failure modes, which are currently not well understood. Phase 2 tests will be used to further understand mass loss rates and modes of both thermal and mechanical failure in composite materials.

The authors exposed 95 samples of aluminum, CFRP, Kevlar fiber-reinforced polymer, GFRP, and sheets of G10 fiberglass to conditions approximating the reentry environment using an inductively coupled plasma (ICP) torch facility. The cylindrical CFRP samples were exposed to the atmospheric pressure plasma, at both the end and the midpoint, to investigate the difference in demisability between parts with exposed edges, like panels, and parts with no edges, such as carbon-overwrapped pressure vessels (COPVs).

In a non-oxidative environment, no composite materials demised within the 5-minute test time. In the oxidative, elevated heat flux environment, CFRP samples demised between 210 s and 270 s. For the first 100 s of insertion time, most of the mass loss was due to pyrolysis of resin, creating an approximately bi-linear mass-loss rate curve with time. In a non-oxidative environment, carbon filaments were observed to unravel from some of the CFRP end-burned samples; however, this effect did not seem to affect the overall time to demise for the samples significantly. These results indicate that both GFRP and CFRP components survive reentry with significantly more remaining mass than current models predict.

1. INTRODUCTION

Human casualty risk from orbital debris reentering the Earth's atmosphere is calculated using one of several tools. U.S. spacecraft that must comply with NASA Standard Practices use the Debris Assessment Software (DAS) package, which uses a simplified conservative version of the higher-fidelity spacecraft reentry model, Object Reentry Survival Analysis Tool (ORSAT), to demonstrate compliance with NASA Standard 8719.14 [2].

ORSAT was developed jointly by the NASA JSC Thermal and Aerosciences Branches and Lockheed in 1993 to predict reentry object behavior, and is currently maintained by the NASA Orbital Debris Program Office.

The current version of the software, ORSAT 6.2, models a reentering spacecraft as a collection of fragments represented as solid shape primitives: spheres, cylinders, boxes, flat plates, flat disks, cones, and rings [3]. The spacecraft is assumed to break up into component fragments at an altitude of 78 km, and ORSAT solves a 3-degrees-of-freedom trajectory equation for each fragment using a 3rd order predictor, 4th order corrector Runge-Kutta integrator. The spacecraft's altitude and velocity from the trajectory equation solution, along with an atmosphere model, are used to calculate the aerodynamic, oxidative, and radiative heat load on the spacecraft fragment.

ORSAT can model a given material as either a standard material or an ablative material. Standard materials are

modeled with a specific heat capacity, thermal conductivity, "melting point" at which the material is assumed to change phase into a form that no longer has any structural integrity and is either vaporized or aerosolized, and a latent heat of fusion. The fragment is considered to have demised when the total integrated heat load absorbed by the material exceeds the sensible thermal capacity, plus the latent heat of fusion. Ablative materials are modeled with an ablation temperature and a best-fit exponential model for recession rate vs. heat flux, and the fragment is considered to have demised when the total recession exceeds the thickness of the material.

While the standard model works well for traditional satellite materials like titanium, aluminum, and well-characterized ablative materials, it is not an accurate representation of the behavior of more complex modern composite materials like carbon fiber-reinforced polymer (CFRP) and glass fiber-reinforced polymer (GFRP).

The standard analysis of these types of materials assumes that the material has a melting point equal to the melting point of the polymer matrix and a thermal capacity and conductivity value equal to that of the bulk material. When the total heat load exceeds the sensible heat capacity of the bulk material plus the latent heat of fusion of the polymer matrix, the material is assumed to have no remaining structural integrity and to immediately shred harmlessly into component fibers.

Several observations of surviving spacecraft fragments, like carbon overwrapped pressure vessels (COPVs) seen in Australia [4], and Brazil [5,6,7], have indicated, however, that this standard model is inadequate, as many carbon fiber overwrapped pressure vessels, a type of debris that previous research had indicated would readily demise [8], have survived mostly intact to the ground [1].

2. EXPERIMENTAL SETUP

2.1. Facility

The authors performed the material demise testing at the ICP torch facility at the University of Texas at Austin. The facility uses a 50 kW induction coil to superheat up to 1.5 g/s of test gas to approximately 6000 K or a specific enthalpy of between 15 and 40 MJ/kg. [9] To insert probes and test articles into the plasma stream, the facility includes a motorized dual-arm water-cooled insertion mechanism.

Small objects, such as spacecraft fragments entering the atmosphere from a ~200 km circular decay orbit, typically experience a peak heat flux between 10 and 80 W/cm^2, depending on the shape and ballistic coefficient of the object. For the shape and size of test articles used in this investigation, the minimum achievable heat flux in the facility was 60 W/cm^2 using air and 30 W/cm^2 using argon as test gasses.

2.2. Facility Modifications

For the current testing, the authors made two major modifications to the facility: an inert gas shroud around the plasma nozzle and a water-cooled flow diverter. The inert gas shroud shielded the sample from entrainment of room air into the plasma stream and allowed for control of the oxygen content to which the sample was exposed. The flow diverter was added because of concerns about molten material dripping down into the plasma chamber, and was used only for test samples where this was a concern.

Because the shape of the test articles was not the standard puck shape, a set of custom mounting arms were constructed to hold the test articles and heat flux probes, pictured in Fig. 1. The sample mounting arm also allowed the sample to be manually rotated during insertion to simulate the tumbling experienced by fragments of a reentering spacecraft.

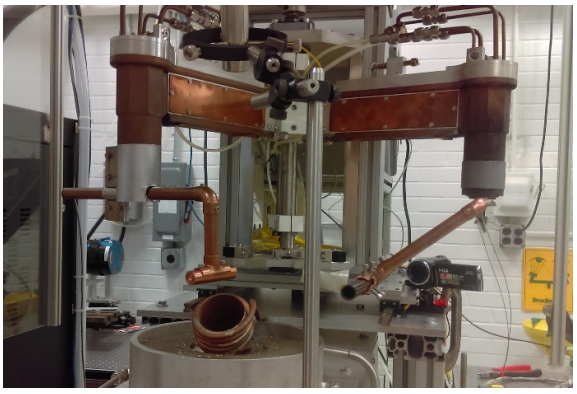

Figure 1. Image of torch facility including inert gas shroud, flow diverter, and probe and test article mounting hardware.

2.3. Test Samples

The authors tested 95 material samples to investigate the effects of fiber material, fiber weave structure, honeycomb core, and oxygen content of the plasma stream on the demisability of composite materials. Tab. 1 lists the material samples used and the shape and fiber weave, if applicable.

Test samples were selected from commercially available materials, which allowed testing a wide range of variables including weave patterns, fiber orientation, and filament density. Material types were selected based on known materials that are commonly used in spacecraft design. This allowed for an efficient and broad test of several variables, with the intent of qualifying the response of materials during thermal loading that currently is not well understood.

Table 1. Test sample descriptions and quantities

Material	Shape	Weave	QTY
Aluminum	Rod	NA	7
Fiberglass	Rod	Unidirectional (axial)	9
Kevlar	Tube	Bi-directional cross-weave	10
Carbon Fiber	Tube	Spiral wound	17
Carbon Fiber	Tube	Bi-directional cross-weave	19
Carbon Fiber	Tube	Planar, unwoven	18
Carbon Fiber	Rod	Unidirectional (axial)	10
G10	Plate	NA	3
CFRP-Al honeycomb	Plate	Bi-directional cross-weave	2

Most of the tests focused on various configurations of CFRP samples since spacecraft fragments made from these materials have been shown, previously, to survive to the ground, contrary to demise predictions [1].

The authors tested four different weave patterns of CFRP:

- twill weave outer wrap with alternating unidirectional layers underneath, as might be used on a CFRP tie-rod,
- bi-directional spiral-wound axial weave similar to the weave pattern of a CFRP over-wrapped pressure vessel,
- alternating planar unidirectional layers as might be used on the face sheet of a honeycomb panel,
- and unidirectional axial fiber rod.

In addition to the composite materials, seven aluminum samples were tested as controls. Previous work has shown that the current reentry demise models work well for heritage materials like steel, titanium, and aluminum, as their primary mode of demise is melting and subsequent aerosolization from aerodynamic shear forces.

2.4. Instrumentation and Measurements

Before each test, the cold-wall heat flux to the sample was measured using a Gardon gauge calorimeter of the approximate size and shape of the sample. For the cylindrical samples, the Gardon gauge was embedded in a copper cylinder with a 0.5 in. diameter and 3 in. length. For the flat plate samples, the Gardon gauge was embedded in a 2 x 3 in. copper plate.

During each test, an infrared pyrometer continuously measured the surface temperature of the sample at the stagnation point of the plasma plume, at a sample rate of approximately 10 Hz. A video camera fitted with a neutral density filter recorded the sample during the test.

During the insertion, the authors measured the total mass loss from each sample by weighing the sample before and after the test using a 200 g scale with an accuracy of ±0.1 g.

The authors measured the mass loss rate as a function of time, for several sample materials, by inserting multiple samples for progressively longer periods. The amount of exposure needed for the material to fully demise was also measured, with total demise defined as the complete destruction of any material within the plasma jet and/or complete structural failure at the stagnation point. Samples that did not reach the demise condition after 5 minutes of exposure to the plasma were considered not to demise, as even objects with extremely high ballistic coefficients only experience peak heating rates for 3 to 4 minutes.

2.5. Test Conditions

The facility operates at atmospheric pressure, which is several times greater than the dynamic pressure experienced by reentering orbital debris. While the heat flux condition could be matched, the oxygen flux condition could not. Instead, the authors chose to bracket the oxidation condition with a fully oxidative (sea-level air plasma) and non-oxidative (sea-level argon plasma) condition. Depending on the shape and ballistic number, a typical spacecraft fragment will see an oxygen density between 0.06% and 8% of that of a sea-level air plasma at a similar temperature (i.e., the oxidative condition used in this test series contains 10 to 1600 times the oxygen flux of a typical reentering fragment).

Many cylindrical samples also were tested at two different points: at the end of the tube and at the midpoint. The end exposure simulated the expected conditions of a carbon fiber panel with free edges that could potentially unravel once the epoxy matrix has been destroyed. The midpoint exposure simulated the conditions of a fragment like a CFRP over-wrapped pressure vessel where the carbon fibers have no edge from which to begin unravelling.

3. PHASE I RESULTS

3.1. Aluminum Samples

The seven aluminum control samples behaved exactly as expected. The samples were considered to have demised when the portion of the sample exposed to the plasma jet lost all structural integrity.

When accounting for the area of the sample actually exposed to the plasma, the measured time to demise is consistent, within a few seconds, with the time calculated based on heat capacity and heat of fusion of

aluminum, as shown in Tab. 2. The predicted demise was estimated by calculating the total sensible heat and latent heat of fusion needed to melt the exposed portion of the sample and dividing this value by the total heating rate, as measured by the Gardon gauge.

Table 2. Comparison of predicted and measured time to demise for aluminum samples

Measured Stagnation Heat Flux (W/cm^2)	Measured Demise (s)	Predicted Demise (s)
87 (air)	27.8	28.9 ± 1.7
94 (air)	22.5	26.7 ± 1.4
87 (air)	29.04	28.9 ± 1.7
24 (argon)	108.4	104.7 ± 21.8
31 (argon)	117.6	81.1 ± 13.1
34 (argon)	107.5	73.9 ± 10.9

The predicted and measured demise in the last two entries in Tab. 2 are not as consistent as the other measurements. This is attributed to inconsistent mounting of the aluminum rod in the sample holder, which could cause differences between the heat flux measured by the Gardon gauge probe and that experienced by the sample.

3.2. Kevlar Fiber Reinforced Polymer

The Kevlar samples demonstrated high demisability, but it is clear from the post-insertion observations pictured in Fig. 2 that the mechanism of demise is pyrolysis and oxidation of the material, rather than phase change.

Figure 2. Charred region of Kevlar sample exposed to plasma

All of the Kevlar samples that were allowed to fully demise did so in less than 35 seconds of exposure. The samples that were exposed to air plasma demised in between 20 and 26 seconds. Fig. 3 shows the failure mechanism of a demised sample.

Figure 3. Kevlar sample exposed until demise

In addition to demise due to oxidation and pyrolysis, the samples were extremely brittle post-test. Many samples structurally failed while being removed from the test fixture. Future tests may be needed to characterize the structural integrity of the samples, but it is clear that any remaining mass would structurally fail due to aerodynamic loading.

3.3. Glass Fiber-Reinforced Polymer

The GFRP rods displayed very different behavior from that of the Kevlar samples. When exposed to a non-oxidizing plasma, the polymer matrix pyrolyzed and was quickly removed from the material. However, the glass fibers remained and slowly melted until the section exposed to the plasma could no longer support the weight at the end of the rod, and the sample was considered to have demised. The result of this test is shown in Fig. 4 and indicates that in the absence of oxidation, the primary mode of demise is melting of the glass fibers, which is consistent with the assumptions made in ORSAT.

Figure 4. Sample of axially oriented GFRP inserted in argon plasma for 80 seconds (considered demised).

In contrast, when the sample is exposed to an oxidative heating environment, as pictured in Fig. 5, there is some melting of the glass fibers, but the primary mode of demise seems to be embrittlement of the glass fiber substrate due to oxidation.

Figure 5. Sample of axially oriented GFRP inserted in air plasma until demise

Based on these results, it is clear that the demisability of GFRP is very sensitive to oxygen content. As Phase 1 testing only was able to characterize the extremes of the oxidation environment, future testing of this material should include a more representative gas mixture to improve GFRP ablation models.

3.4. Carbon Fiber Reinforced Polymer

Three of the four CFRP weave patterns were exposed to argon plasma for incrementally longer periods of time to measure the total mass loss of the sample as a function of exposure time. Figs. 6 and 7 show the mass loss in tubes of these three weave patterns in an argon and air plasma, respectively. The amount of mass in the section of tube exposed to the plasma is approximately 4.5 g. Fig. 8 shows the mass loss as a percentage of the approximate exposed mass.

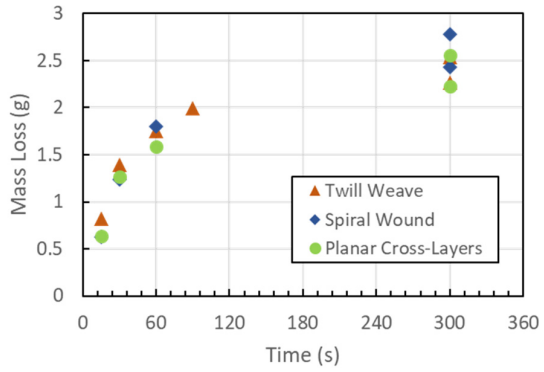

Figure 6. Mass loss of CFRP tubes in argon plasma

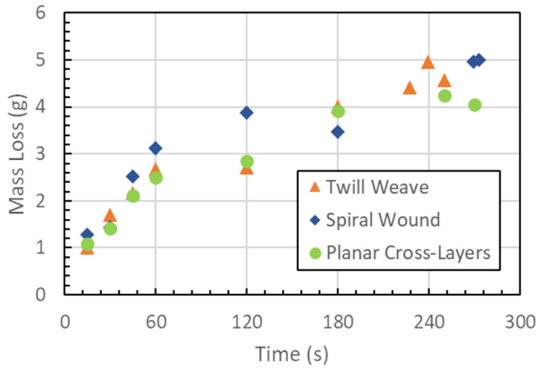

Figure 7. Mass loss of CFRP tubes in air plasma

In both oxidation cases, the mass loss is initially rapid, losing 2 to 3 g in the first minute of exposure, and then losing only approximately 1 g in the four following minutes of exposure. As seen in Figs. 7 and 8, the mass loss follows a bilinear trend with time. This seems to be caused by the initial rapid charring of the epoxy resin, followed by the much slower process of ablation of the carbon char products and fiber substrate.

Samples that were not exposed to an oxidative heating environment did not achieve demise within the allotted 5-minute test time. This is not surprising, as without oxidation, the main mode of material removal for a pure carbon material is through sublimation, which is not a dominant process until the surface of the material reaches a temperature of approximately 3000 K. In all of the tests, the maximum surface temperature of the samples reached approximately 1500 K.

When the mass loss in each sample is shown as a percentage of the approximate total mass exposed directly to the plasma, as in Fig. 8, the variation between types of weave decreases significantly, especially in the first 60 seconds of exposure, and makes the bilinear nature of the process even more evident.

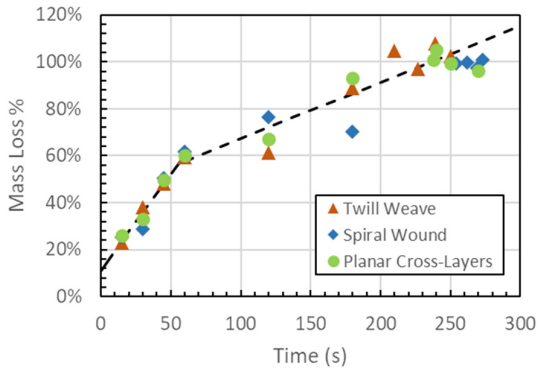

Figure 8. Mass loss of CFRP tubes in air plasma as percentage of mass directly exposed to plasma

Linear regression obtained a slope of 0.82% per second mass loss in the first phase, and a slope of 0.24% per second mass loss in the second phase. The fact that the sharp change in mass loss rate occurs at around 60% mass loss indicates that most, if not all, of the epoxy matrix within the sample is removed in the first 60 seconds of exposure, and the 71% reduction in mass loss rate after this time is due to the comparatively slow carbon ablation process. This result is consistent with observed surviving CFRP orbital debris fragments; much of the epoxy is removed from the material, leaving a mass of interwoven carbon fibers [4,6,7].

Some difference also can be seen in the time to demise of the different fiber weave patterns. Twill weave demised the fastest and the helical wound demised the slowest, with a difference of up to 30 s between the two, as shown in Fig. 9. Some of this difference is due to variability in the size of the samples. The total starting mass of different samples varied by up to 3% within the weave categories, and the spiral wound samples had a 10% higher starting mass than the other two types of samples.

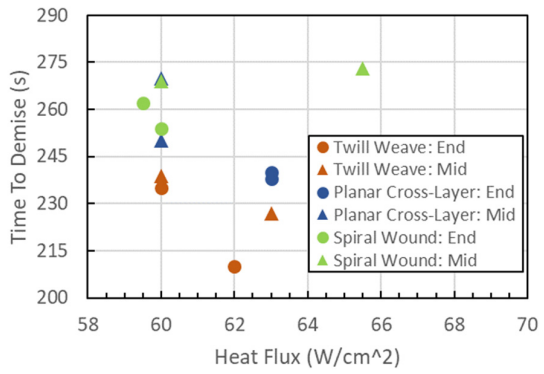

Figure 9. Time to demise for CFRP tubes in air

3.5. CFRP Face Sheet/Aluminum Honeycomb

Another frequently used material in spacecraft construction is a composite panel with CFRP face sheets sandwiching an aluminum honeycomb panel. Two samples of this material were tested to demise to obtain qualitative observations of failure modes in the material and the degree to which the carbon fiber exterior insulates the internal aluminum from melting.

Fig. 10 shows the progression from initial insertion to demise of the windward face sheet and honeycomb layer of a sample of CFRP/Aluminum honeycomb composite panel. The sample is 7 mm thick with approximately 0.5-mm-thick face sheets.

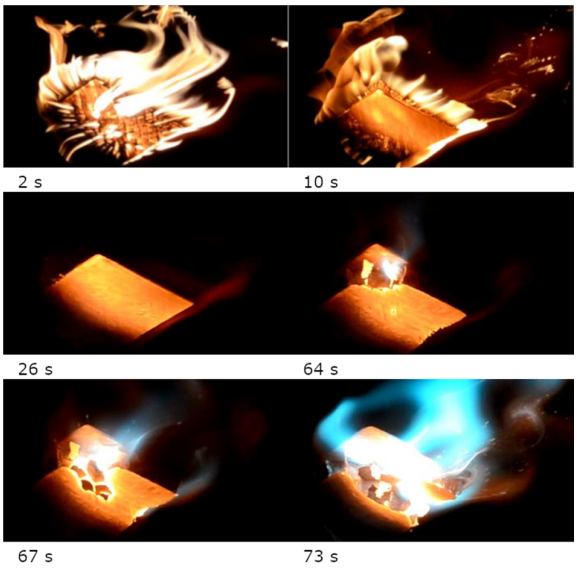

Figure 10. Progression of demise in aluminum honeycomb/CFRP face sheet sample

Immediately after insertion, the epoxy matrix begins pyrolysis, releasing volatile gases visible in the first two images as sooty flames. By 26 seconds of exposure, all of the epoxy matrix has pyrolyzed and the carbon fibers are slowly ablating. At 64 seconds, the final layer of fibers have begun to ablate and expose the internal honeycomb layer. It is clear from the images at 64 seconds and 67 seconds that the aluminum honeycomb is still mostly intact; it doesn't appear to begin demise until it is exposed directly to the plasma by the ablation of the face sheet, and until that time is relatively insulated from the surrounding environment by the carbon fibers.

This appears to contradict the findings of Masuoka, et al. [8] and shows that a low-melting point material enclosed by a CFRP overwrap may not readily demise as the CFRP can provide an effective thermal protection barrier for the weaker interior material.

4. MODELING

These results showing much greater survivability of CFRP materials prompted the development of a new material model [10] that could be implemented in the current ORSAT 6.2, but would capture the behavior observed in these tests and in other recent arcjet tests [1].

ORSAT 6.2 allows a fragment to be modeled as a composite material consisting of several material layers. The updated CFRP model uses this feature to simulate the CFRP material as two separate material layers: an external pseudo-epoxy layer that is removed by pyrolysis and an internal pseudo-carbon layer that largely remains intact.

The underlying assumption of this two-material model is that all of the epoxy will pyrolyze and be removed from the composite, but this removal will have minimal impact on the overall thickness of the composite—currently modeled as a 5% reduction in wall thickness.

The material properties of each component are calculated based on the volume of the fragment and the epoxy fraction by mass, and tuned to match the original heat capacity and thermal conductivity of the overall CFRP composite. The equations for the specific heat capacity and thermal conductivity of the CFRP composite used in ORSAT are given in Eq. (1) and Eq. (2) below. The constant material properties for the pseudo-epoxy and pseudo-carbon are given in Tab. 3.

$$C_{p,CFRP}(T) = 10.726 + 2.7539 * T \quad (1)$$

$$k_{CFRP}(T) = 0.4224 + 3.7669 * 10^{-4} * T \quad (2)$$

The density of the epoxy and carbon components is dependent on the volume of each phase and is calculated using the Eq. -3-10.

$$V_{CFRP} = V(shape, L, W, H, t) \quad (3)$$

$$\delta t = 0.05t \quad (4)$$

$$V_C = V(shape, L, W, H, t - \delta t) \quad (5)$$

$$V_E = V_{CFRP} - V_C \quad (6)$$

$$M_{CFRP} = V_{CFRP}\, \rho_{CFRP} \quad (7)$$

$$M_E = M_{CFRP} - M_E \quad (8)$$

$$\rho_C = \frac{M_C}{V_C} \quad (9)$$

$$\rho_E = \frac{M_E}{V_E} \quad (10)$$

Table 3. Constant material property values for epoxy and carbon components of CFRP material model

Property	Epoxy	Carbon
Emissivity	0.9	0.9
Melting Point (K)	700	3915
Latent Heat of Fusion (J/kg)	2326	9999999
Oxide Heat of Formation (J/kg-O_2)	12305781	0

The density values given in Eq. (9) and Eq. (10) are then used to calculate the specific heat of the pseudo-epoxy and pseudo-carbon components by applying density weighting to the $C_{p,CFRP}$ value given in Eq. (1). These density-weighted specific heats are given in Eq. (11) and (12) below.

$$C_{p,C}(T) = \frac{\rho_{CFRP}}{\rho_C} C_{p,CFRP}(T) \quad (11)$$

$$C_{p,E}(T) = \frac{\rho_{CFRP}}{\rho_E} C_{p,CFRP}(T) \quad (12)$$

5. CONCLUSIONS

Testing of multiple materials in an oxidative and non-oxidative plasma environment similar to reentry conditions showed that composite materials with refractory material fiber reinforcement like carbon fiber are much less likely to demise on reentry than current models predict. Tests of aluminum samples validated existing ORSAT models and therefore, do not justify any changes.

Tests of Kevlar show that the material readily demises during representative thermal loading alone. Additionally, test samples show minimal residual structural integrity that would further decrease the survivability of the material during reentry due to anticipated aerodynamic loads. Further testing of Kevlar is recommended at a lower priority than other materials, since the lack of structural integrity means it is likely a low risk of human casualty.

CFRP materials, in particular, survive more than 5 minutes of exposure to peak heat loads, indicating that significant portions of spacecraft fragments composed of these materials will likely survive reentry under most circumstances, possibly with enough kinetic energy to pose human casualty risk.

In the CFRP and GFRP samples, the epoxy matrix is first removed through pyrolysis, leaving only the fiber substrate and residual carbon. With thick-enough layups, the remaining fibers could act to shield interior portions of the material from further pyrolysis, slowing demise even further, though none of the samples in this test were thick enough to test this possibility. Kevlar samples appeared to show concurrent pyrolysis of both the fibers and the matrix, completely demising within a relatively short period of time.

The CFRP samples also maintained significant structural integrity after complete pyrolysis of the epoxy matrix. Samples exposed to the plasma at the midpoint of the cylinder exhibited no motion in the cantilevered section until a significant portion of the sample wall had ablated completely.

Manipulation of partially ablated samples did, however, show that some minimal application of bending moment could cause the sample to flex at the plasma application point, indicating a significant but yet unmeasured loss

of structural integrity. Further work is required to determine how much force might be necessary to cause aerodynamic shredding of partially ablated CFRP.

6. FUTURE WORK

This work highlights the need for further development of a more accurate model for the demise of CFRP components of a re-entering spacecraft. A simple transition model has been developed, but a more complete model will need to include pyrolysis and ablation rates of both the epoxy and carbon fiber components, as well as a force model to calculate aerodynamic shredding of the bare carbon fibers.

Phase II testing is currently planned for the summer of 2019 and will focus on obtaining strength measurements of CFRP samples after various exposure times and heating rates, more detailed mass loss and pyrolysis rates, and thermal conductivity of the charred material. These data will then be used to develop a more detailed model of not only ablation and demise of the CFRP and GFRP material itself, but also its interaction with other materials in complex composite structures like COPVs and aluminum honeycomb composite panels.

REFERENCES

1. Lips, T., et al. (2016). "About the Demisability of Propellant Tanks During Atmospheric Re-Entry from LEO." Paper presented at the 8th IAASS Conference, Melbourne, FL, USA.
2. NASA-STD-8719.4a. (2011). "Process for Limiting Orbital Debris". Retrieved from: https://standards.nasa.gov/standard/nasa/nasa-std-871914
3. Smith, R. N., et al. (2006). "Object Reentry Survival Analysis Tool (ORSAT) – Version 6.0." JSC-62861. Houston, TX: NASA Lyndon B. Johnson Space Center.
4. Grubel, James. (2008). "Australian farmer finds mystery space junk." *Reuters*. Retrieved from: https://www.reuters.com/article/us-australia-spacejunk/australian-farmer-finds-mystery-space-junk-idUSSYD8466320080328
5. Bacon, John B., personal communication, Feb. 4, 2019.
6. Plait, Phil. (2008). "What Object Fell on Brazil?" *Discover Magazine* (blog). Retrieved from: http://blogs.discovermagazine.com/badastronomy/2008/03/25/what-object-fell-on-brazil/
7. Campos Jr., Ricardo. (2012). "Objeto que caiu em chácara é tanque de combustível estrangeiro, diz AEB." *Campo Grande News*. Retrieved from: https://www.campograndenews.com.br/cidades/objeto-que-caiu-em-chacara-e-tanque-de-combustivel-estrangeiro-diz-aeb
8. Masuoka, T., Masuda, I., and Kajiwara, K. (2013). "Demise Characteristics Evaluation for Melting Promotion Type Tank." Paper presented at the 49th AIAA/ASME/SAE/ASEE Joint Propulsion Conference, San Jose, CA.
9. Greene, B.R., Clemens, N.T., and Varghese, P.L. (2017). "Characterization of a 50 kW Inductively Coupled Plasma Torch for Testing of Ablative Thermal Protection Materials." Paper presented at the 55th Aerospace Sciences Meeting, Grapevine, TX.
10. Ostrom, C. (2019). "Implementation of the Two-Material CFRP Model in ORSAT" Internal memo. Orbital Debris Program Office.